



# Spectral width reduction using apodized cascaded fiber Bragg grating for post-dispersion compensation in WDM optical networks

Ahmed F. Sayed<sup>1</sup> · Fathy M. Mustafa<sup>2</sup> · Ashraf A. M. Khalaf<sup>3</sup> · Moustafa H. Aly<sup>4</sup>

Received: 22 April 2019 / Accepted: 27 January 2021 / Published online: 6 March 2021  
© The Author(s), under exclusive licence to Springer Science+Business Media, LLC part of Springer Nature 2021

## Abstract

This paper proposes a system that aims to reduce the spectral width,  $\Delta\lambda$ , of the optical signal at transmitter for WDM system over distance 100 km. Also, a chirped fiber Bragg grating (CFBG) at the receiver is used to compensate dispersion. The proposed system consists of four cascaded FBGs connected between light source and optical fiber. Many apodization functions are investigated to enhance the performance of the FBG in the proposed system, and  $\Delta\lambda$  is obtained at every stage and apodization function. The Q-factor and bit error rate (BER) are obtained at distances 30, 40 and 50 km. It is found that Cauchy apodization function is the best one that reduces the reflective spectral width,  $\Delta\lambda$ , and achieves a maximum Q-factor and minimum BER at distances 30, 40 and 50 km at the last stage.

**Keywords** Apodization · BER · Fiber Bragg grating · Q-factor · Spectral width

## 1 Introduction

Narrowing the spectral linewidth of laser diodes is playing an important role in optical communication systems [1, 2]. There are some applications need laser sources with a narrow line width, a high degree of coherence and low optical phase noise.

Some applications such as gravitational wave detectors, formation-flying satellites and length stabilized fiber

distribution systems, require coherent lasers to detect small length changes over hundreds of distances [3–5]. In a multiple quadrature amplitude modulations (QAM), it is important to have a laser source with a narrow spectral line width to have an acceptable bit error rate (BER) [6]. Another type of application needs a narrow linewidth like WDM optical communication systems to reduce dispersion phenomena. When a light source emits a wavelength with line width ranges  $\Delta\lambda$ , they propagate along the optical fiber with different velocities and get received at different times causing dispersion. Dispersion is considered as an important limiting factor for data transmission. It is the phenomenon that causes the expansion of the light pulse as it propagates through the fiber and limits transmission capacity whether the system is digital or analog. The dispersion effect is different in multimode and single-mode fibers [7]; also bit rates, signal-to-noise ratio (OSNR) and performance of the WDM communication system are affected and limited by it [8, 9]. Some optical tools have been invented to reduce the line width of laser sources like fiber Bragg grating (FBG). FBG laser has been used on erbium-doped lasers due to their potential in communication and sensor applications [10]. Many types of research have been done to reduce the linewidth of laser sources. In [11], a narrow line width terahertz (THz) generation using a cascaded Brillouin fiber laser structure and a uni-travelling carrier photodiode is investigated. The use of

✉ Ashraf A. M. Khalaf  
ashkhalaf@yahoo.com

Ahmed F. Sayed  
ahmed.darwesh.te@gmail.com

Fathy M. Mustafa  
fmmg80@eng.bsu.edu.eg

Moustafa H. Aly  
mosaly@aast.edu

<sup>1</sup> Transmission Department, Telecom Egypt Company, Fayoum, Egypt  
<sup>2</sup> Electrical Engineering Department, Faculty of Engineering, Beni-Suef University, Beni-Suef, Egypt  
<sup>3</sup> Electrical Engineering Department, Faculty of Engineering, Minia University, Minia, Egypt  
<sup>4</sup> Electronics and Communications Engineering, College of Engineering and Technology, Arab Academy for Science, Technology and Maritime Transport, Alexandria, Egypt

the cascaded Brillouin laser greatly increases the line width reduction factor compared to a single Brillouin laser structure. The line width of the realized THz source is found to be  $< 100$  Hz at 1014.7 GHz without the use of any active stabilization of the laser cavity or any microwave reference. In [12], the spectral line width of a laser source by direct phase noise compensation is proposed and demonstrated experimentally. Phase noise compensation is achieved by simply applying an error signal to an external phase modulator, where the error signal is generated to keep the same power level for the detected in and quadrature signals. It is found that the spectral line width of the laser is reduced significantly from 450 to 60 kHz. In [13], the effect of the particular frequency noise spectrum of such a laser is analyzed on its degree of coherence, its line width and the resulting interferometric noise. The laser linewidth computed from the power spectral density of frequency noise of the laser is reduced from 570 kHz down to an equivalent of 1.8 kHz when the output signal is observed for 30 ms and from 370 kHz to 18 Hz for 1 ms. In [14], a compact structure has been proposed based on the FP cavity incorporating a built-in wavelength detuned band-pass filter. The designed structure is simulated by the broadband optical traveling wave model. Simulation results show that this design is able to narrow the optical spectrum significantly from 16 nm to around 8 nm and the  $-20$  dB bandwidth is decreasing slightly with the increase in the detuning until around 3.2 nm and the adjacent pass-band starts to acquire sufficient gain within the gain bandwidth and take effect on broadening the bandwidth with further increase in the detuning. In [15], a mechanical and actuation performance was characterized using copper aluminum manganese nickel shape memory alloy coatings. The obtained results could be used as a guide to design thermally actuated optical fiber towards application oriented requirements. In [16] presents a widely tunable narrow-linewidth semiconductor laser using a ring-resonator based mirror as the extended cavity. They presented two generations of lasers. The first-generation lasers showed an intrinsic linewidth of  $\sim 2$  kHz, and the second achieved an intrinsic linewidth below 220 Hz. In [17], fully integrated extended distributed Bragg reflector (DBR) laser with  $\sim 1$  kHz linewidth and over 37 mW is demonstrated. Long Bragg grating with narrow bandwidth (2.9 GHz) is essential to reduce the laser linewidth while maintaining high output power and single-mode operation.

This paper aims to reduce the spectral width of the light source,  $\Delta\lambda$ , that reaches different parts of the communication link. This is one of the delay parameters which cause dispersion for the optical signal. Firstly, dispersion is reduced at the transmitter by the apodized FBGs cascaded model, and secondly, it is compensated at the receiver by the CFBG as a post-compensator. To achieve that, a

proposed model consists of multistages apodized FBGs to reduce the spectral width,  $\Delta\lambda$ , of the output reflected wavelength before transmitting in the optical fiber.

Depending on the proposed system, (1) bit rate-distance product for single mode fiber can be increased up to (Tb/s).km and (2) increase performance of WDM communication system.

This paper is organized as follows. The basic model and analysis are discussed in Sec. II. In Sec. III, we present the proposed system. Sect. IV displays and discusses simulation results. Sec. V displays the proposed model evaluation. Finally, Sec. VI is devoted to the main conclusions.

## 2 Basic model theory and analysis

In this section, definitions equations for CFBG, optical signal-to-noise ratio (OSNR), Q-factor and the bit error rate (BER) are explained. Different apodization functions which are applied to CFBG to improve its performance in dispersion compensation are illustrated.

### 2.1 Chirped fiber Bragg grating

In this section, some definition equations and some apodization functions for CFBG are illustrated as in Fig. 1. The Bragg wavelength along the core of the CFBG,  $\lambda_B(z)$ , and the refractive index,  $n(z)$ , are given by [10, 18]:

$$\lambda_B(z) = 2n(z)\Lambda(z) \quad (1)$$

$$n(z) = n_{\text{eff}} + \Delta n g(z) \cos \left\{ \frac{2\pi z}{\Lambda_0} (1 + xz) \right\} \quad (2)$$

where  $x$  is the chirp parameter of the grating and  $g(z)$  is the apodization function.

There are many apodization functions used to improve performance of FBG and CFBG. In this paper, we use the following apodization functions [19–21]:

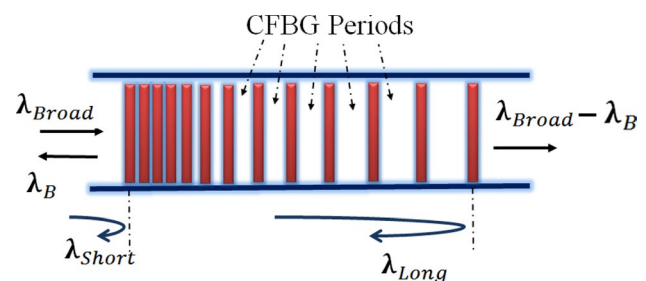


Fig. 1 Schematic diagram of a chirped grating

**2.1.1 Blackman**

$$g(z) = \left[ \frac{1 + 1.19 \cos(x) + 0.19 \cos(2x)}{2.38} \right] \tag{3}$$

$$x = \left[ \frac{2\pi(z - \frac{L}{2})}{L} \right], 0 < z < L \tag{4}$$

**2.1.2 Cauchy**

$$g(z) = \left[ \frac{1 - \left( \frac{2(z - \frac{L}{2})}{L} \right)^2}{1 - \left( \frac{2C(z - \frac{L}{2})}{L} \right)^2} \right] \tag{5}$$

where  $C = 0.5, 0 < z < L$ .

**2.1.3 Sinc**

$$g(z) = \left[ \frac{A \sin(x)}{x} \right] \tag{6}$$

$$x = \left[ \frac{2\pi(z - \frac{L}{2})}{L} \right], 0 < z < L \text{ and } A = 3 \tag{7}$$

**2.1.4 Tanh**

$$x = \tanh\left(\frac{4z}{l}\right) \tanh\left(\frac{4(1-z)}{l}\right), 0 < z < L \tag{8}$$

**2.1.5 Hamming**

$$g(z) = \left[ \frac{1 + H \cos\left(\frac{2\pi(z - \frac{L}{2})}{L}\right)}{1 + H} \right] \tag{9}$$

where  $H = 0.9, 0 < z < L$ .

**2.1.6 Gaussian**

$$g(z) = \exp\left(-a\left(\frac{z}{l} - 0.5\right)^2\right) \tag{10}$$

where  $a = 1, 0 < z < L$ .

The spaces between planes along grating are [21]:

$$\Lambda(z) = \Lambda_0 + xz \tag{11}$$

where  $\Lambda_0$  is the first space on the core,  $x$  is the linear chirp or slope and  $\Delta\lambda$  is the chirp between two ends of the grating is given by [23]:

$$\Delta\lambda = 2n_{\text{eff}}(\Lambda_{\text{long}} - \Lambda_{\text{short}}) \tag{12}$$

where  $\Lambda_{\text{long}}$  is the longest period and  $\Lambda_{\text{short}}$  the shortest period inside CFBG core. The time delay,  $\tau$ , for each wavelength along CFBG can be calculated by [23]:

$$\tau(\lambda) = (\lambda_B - \lambda) \frac{2n_{\text{eff}} l}{\Delta\lambda c} \tag{13}$$

where  $c$  is the speed of light in the vacuum and  $l$  is the grating length.

The dispersion of the CFBG,  $D_g$ , can be obtained as [10]:

$$D_g = \frac{2n_{\text{eff}} l}{\Delta\lambda c} \tag{14}$$

**2.2 OSNR, Q-factor and BER**

The relation between OSNR and the total dispersion can be calculated from previous work as in [19], where loss due to splices and connectors can be neglected related to optical fiber loss:

$$\text{OSNR} = \frac{P_{\text{in}} D_f}{N_f h\nu \Delta\nu_0 \alpha (D_t + D_g)} \tag{15}$$

where  $P_{\text{in}}$  is the input power,  $N_f$  is the amplifier noise figure,  $h$  is Planck’s constant,  $\nu$  is the frequency,  $\Delta\nu_0$  is the bandwidth frequency,  $D_f$  is the dispersion coefficient of the optical fiber,  $D_t$  is the total dispersion over the optical fiber,  $D_g$  is the CFBG dispersion and  $\alpha$  is the attenuation coefficient of the optical fiber. The relation between Q-factor and OSNR is [8]:

$$Q = \frac{\text{OSNR}}{\sqrt{2 \text{OSNR} + 1}} \sqrt{\frac{B_o}{B_c}} \tag{16}$$

where  $B_o$  is the optical bandwidth of the optical filter and  $B_c$  is electrical bandwidth of the receiver filter.

BER is a function of Q-factor and is expressed by:

$$\text{BER} = 0.5 \operatorname{erfc}\left(\frac{Q}{\sqrt{2}}\right) \tag{17}$$

### 3 The proposed system

This section is divided into subsections. The first section presents the proposed system mathematical model and its derivation, and the second section presents the use of the proposed system in a WDM network.

#### 3.1 Mathematical Model

The proposed system aims to reduce  $\lambda$  of the light source using cascaded FBGs. It consists of four cascaded FBGs with four stages. The reflectivity of each stage is derived related to of the first stage. Figure 2 shows four identical cascaded FBGs, where the reflected signal of each stage is the input signal for the new stage.

#### 4 First stage FBG

The parameters of the first stage are defined as  $X_{01}$  the incident optical signal,  $Y_{01}$  the reflected optical signal and  $X_{11}$  the output optical signal. The reflected optical signal at the output of the grating is equal to zero. Therefore, the transfer matrix can be written as:

$$\begin{bmatrix} X_{01} \\ Y_{01} \end{bmatrix} = \begin{bmatrix} T_{11} & T_{12} \\ T_{21} & T_{22} \end{bmatrix} \begin{bmatrix} X_1 \\ 0 \end{bmatrix} \tag{18}$$

So,

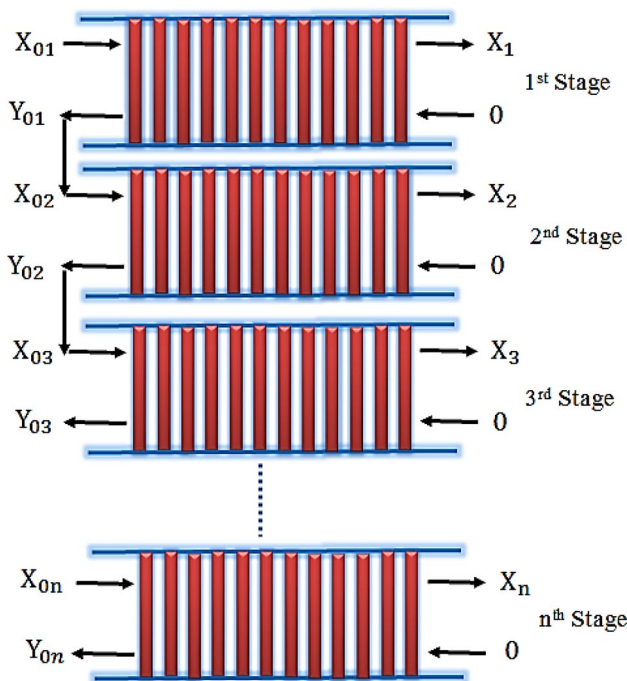


Fig. 2 N stages for cascaded FBGs

$$X_{01} = T_{11}X_1 \tag{19}$$

$$Y_{01} = T_{21}X_1 = \frac{X_{01}T_{21}}{T_{11}} \tag{20}$$

Then, the reflectivity of the first stage,  $R_{01}$ , is obtained as:

$$R_{01} = |\rho_{01}|^2 \tag{21}$$

where

$$\rho_{01} = \frac{Y_{01}}{X_{01}} = \frac{T_{21}}{T_{11}} \tag{22}$$

#### 5 Second stage FBG

In this case, the reflected optical signal of the first FBG is connected as the input signal of second FBG, which has the same T matrix of the first FBG. The reflectivity of the two FBG stages can be calculated as:

$$\begin{bmatrix} X_{02} \\ Y_{02} \end{bmatrix} = \begin{bmatrix} T_{11} & T_{12} \\ T_{21} & T_{22} \end{bmatrix} \begin{bmatrix} X_2 \\ 0 \end{bmatrix} \tag{23}$$

where  $X_{02}$  is the incident optical signal at second stage,  $Y_{02}$  is the reflected optical signal second stage and  $X_2$  is the output optical signal second stage. In this case:

$$X_{02} = Y_{01} = X_{01} \frac{T_{21}}{T_{11}} \tag{24}$$

$$\begin{bmatrix} X_{01} \frac{T_{21}}{T_{11}} \\ Y_{02} \end{bmatrix} = \begin{bmatrix} T_{11} & T_{12} \\ T_{21} & T_{22} \end{bmatrix} \begin{bmatrix} X_2 \\ 0 \end{bmatrix} \tag{25}$$

$$X_{01} \frac{T_{21}}{T_{11}} = T_{11}X_2 \tag{26}$$

Then,

$$X_{01} = \frac{(T_{11})^2}{T_{21}} X_2 \tag{27}$$

$$Y_{02} = T_{21}X_2 \tag{28}$$

Hence, the reflectivity,  $R_{02}$ , for the second stage is:

$$R_{02} = |\rho_{02}|^2 = \left| \frac{Y_{02}}{X_{01}} \right|^2 = (R_{01})^2 \tag{29}$$

where

$$\rho_{02} = \frac{Y_{02}}{X_{01}} = \left(\frac{T_{21}}{T_{11}}\right)^2 = (\rho_{01})^2 \tag{30}$$

### 6 Third stage FBG

The output of second FBG,  $X_{02}$ , is equal to input  $X_{03}$  of third FBG, where  $X_{03}$  is the incident optical signal at third stage,  $X_{02}$  is the reflected optical signal second stage and  $X_3$  is the output optical signal third stage. In this case:

$$X_{03} = Y_{02} = X_{01} \left(\frac{T_{21}}{T_{11}}\right)^2 \tag{31}$$

$$\begin{bmatrix} X_{01} \left(\frac{T_{21}}{T_{11}}\right)^2 \\ Y_{03} \end{bmatrix} = \begin{bmatrix} T_{11} & T_{12} \\ T_{21} & T_{22} \end{bmatrix} \begin{bmatrix} X_3 \\ 0 \end{bmatrix} \tag{32}$$

$$X_{01} \left(\frac{T_{21}}{T_{11}}\right)^2 = T_{11} X_3 \tag{33}$$

$$X_{01} = \frac{(T_{11})^3}{(T_{21})^2} X_3 \tag{34}$$

$$Y_{03} = T_{21} X_3 \tag{35}$$

We can calculate the reflectivity,  $R_{03}$ , for the third FBG by:

$$R_{03} = |\rho_{03}|^2 = \left|(\rho_{01})^3\right|^2 = (R_{01})^3 \tag{36}$$

where

$$\rho_{03} = \frac{Y_{03}}{X_{01}} = \left(\frac{T_{21}}{T_{11}}\right)^3 \tag{37}$$

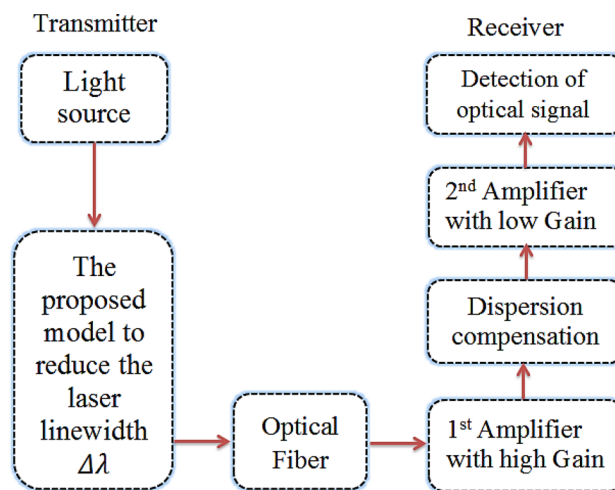


Fig.3 Block diagram to improve WDM system performance

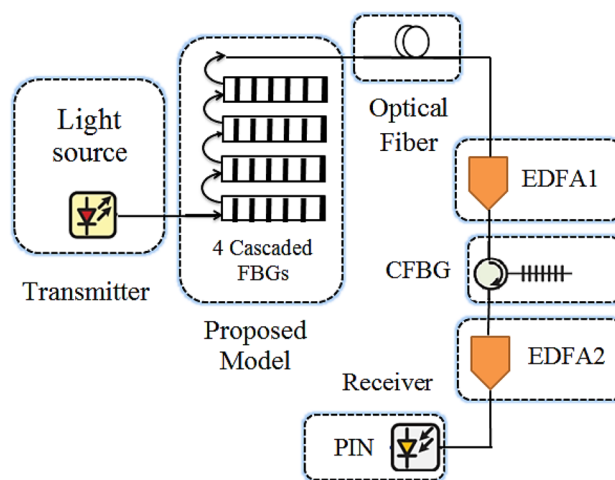


Fig.4 Proposed system in a WDM optical link

### 7 nth stage FBG

According to previous discussion, for the  $n$ th stage, the reflectivity  $R_{0n}$  can be calculated as:

**Table 1** WDM link parameters

| Parameter  | Value | Unit     |
|--|-------|----------|
| Input power  | +5    | dBm      |
| Dispersion   | 17    | ps/nm.km |
| Bit rate   | 10    | Gp/s     |
| Attenuation  | 0.25  | dB/km    |
| Fiber length   | 100   | Km       |
| $B_o/B_c$  | 16    | -        |
| $\Delta\nu_0$ Frequency range                              | 4     | THz      |
| EDFA1 amplifier at receiver with noise Fig. 8 dB with gain | 10    | dB       |
| EDFA2 amplifier at receiver with noise Fig. 8 dB with gain | 5     | dB       |

$$R_{0n} = (R_{01})^n \quad (38)$$

Similarly, for cascaded FBGs of the same parameters

**Table 2** FBG parameters

| Parameter                  | Value | Unit |
|----------------------------|-------|------|
| CFBG grating length        | 20    | Mm   |
| Frequency                  | 193.1 | THz  |
| Effective refractive index | 1.45  | -    |
| Induced refractive index   | 1E-4  | -    |

**Table 3** CFBG parameters

| Parameter                  | Value     | Unit |
|----------------------------|-----------|------|
| CFBG grating length        | 2 mm      | Mm   |
| Frequency                  | 193.1 THz | THz  |
| Effective refractive index | 1.45      | -    |
| Induced refractive index   | 7E-5      | -    |

and each of a reflectivity  $R$ , the reflectivity of all  $n$  groups is equal to  $(R)^n$ .

## 7.1 The proposed system in WDM network

Figure 3 shows block diagram to show how our system can improve the performance of the WDM system. At transmitter, the model is connected to the light source to decrease the spectral width  $\Delta\lambda$  of the output optical signal. At receiver, the optical signal is amplified with high gain first amplifier before compensating the dispersion. The second amplifier with low gain amplifies the optical signal after dispersion compensation and before detection of optical signal. Figure 4 shows the conversion of the block into a real WDM network with its optical component in each stage. At transmitter, a light source with output power 5 dBm and bit rate 10 GB/s is connected to the model with only 4 cascaded FBG. The proposed model reduces the spectral width of the optical signal and feeds it to the optical fiber with length 110 km. At receiver, an erbium-doped fiber amplifier (EDFA1) with gain 10 dB amplifies the optical signal and feeds it to CFBG to compensate dispersion.

EDFA2 with gain 5 dB amplifies the optical signal after dispersion compensation process. A PIN photodiode detects the optical signal and converts it into electrical signal. Table 1 shows the WDM system parameters that are used within the proposed system.

Tables 2 and 3 show the FBG and CFBG parameters used in the proposed system.

## 8 Simulation results and discussion

Based on the described model, a MATLAB code is performed. The simulation is done with the six mentioned apodization functions. The best results are found and displayed in Blackman, Cauchy and Sinc in terms of reflectivity  $R$ , reflected spectral width  $\Delta\lambda$  (nm), Q-factor and BER.

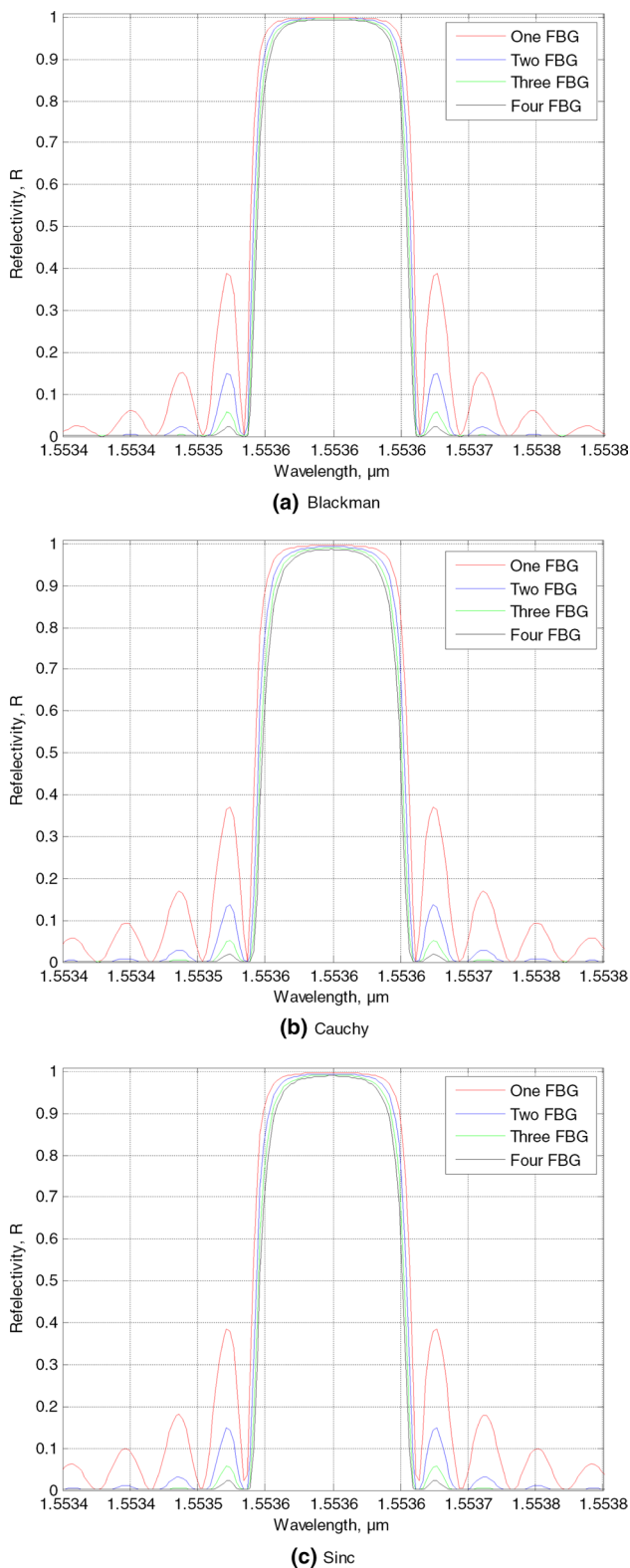


**Fig.5** Cascaded reflectivities of **a** Blackman, **b** Cauchy and **c** Sinc apodization functions

**Table 4** Reflectivity and the spectral width after each stage

|          |                            | 1st    | 2nd    | 3rd    | 4th    |
|----------|----------------------------|--------|--------|--------|--------|
| Blackman | R                          | 0.998  | 0.9976 | 0.9963 | 0.9951 |
|          | $\Delta\lambda(\text{nm})$ | 0.120  | 0.116  | 0.113  | 0.111  |
| Cauchy   | R                          | 0.9966 | 0.9932 | 0.9898 | 0.9864 |
|          | $\Delta\lambda(\text{nm})$ | 0.113  | 0.108  | 0.104  | 0.102  |
| Sinc     | R                          | 0.9973 | 0.9947 | 0.992  | 0.9894 |
|          | $\Delta\lambda(\text{nm})$ | 0.116  | 0.111  | 0.108  | 0.106  |

### 8.1 Relectivity

Figure 5 displays the reflectivity after each stage of the four cascaded FBG stages.  $\Delta\lambda$  the spectral width of the reflected optical signal, reflectivity R and the side lobes are observed at every stage.

As in Fig. 5b, the relation between the reflectivity and the reflective wavelength for Cauchy apodization function is shown. The transfer matrix T transferred from one FBG gives the red curve and  $\Delta\lambda$  as shown. After stage one, it transfers to the stage two and the output as in blue curve where  $\Delta\lambda$  gets narrower. Also, the same for Sect. 3 or stage three the output in green curve and  $\Delta\lambda$  gets narrower than stages one and two.

The simulation results show that the reflectivity R is decreased at every stage until it is equal 0.9951 for Blackman, 0.986 for Cauchy and 0.9894 for Sinc at the last stage.  $\Delta\lambda$  the spectral width of the reflected optical signal is also decreased at every stage where it decreases to 0.111 nm for Blackman, 0.102 nm for Cauchy and 0.106 nm for Sinc at the last stage. The side lobes around the main lobes are reduced from a stage to another. At the last stage, the side lobes are nearly very small for all apodization functions. Table 4 summarizes the obtained results for reflectivity and spectral width at all FBG stages. It is found that at the last stage, Blackman gives the best reflectivity 0.9951. The best reduced  $\Delta\lambda$  (nm) is obtained from Cauchy.

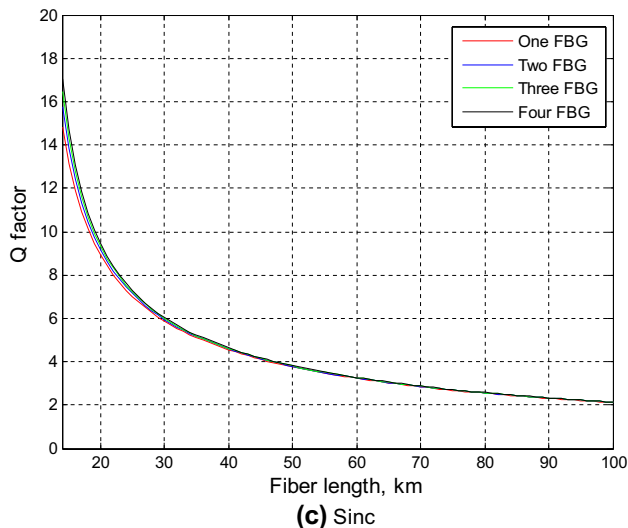
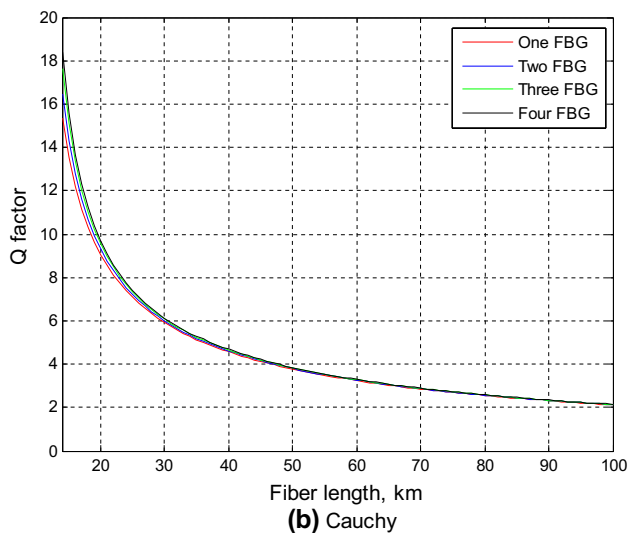
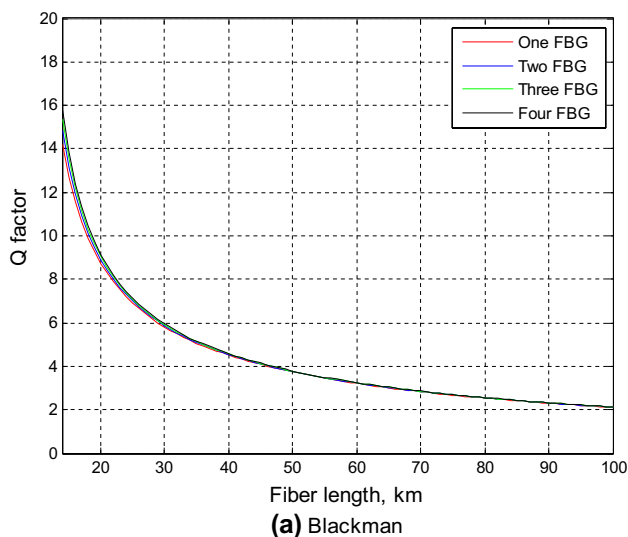


**Fig.6** Q-factor after each stage for **a** Blackman, **b** Cauchy and **c** Sinc apodization functions

**Table 5** Q-factor results

|                 | Distance (km) | 1st   | 2nd   | 3rd   | 4th   |
|-----------------|---------------|-------|-------|-------|-------|
| <b>Blackman</b> |               |       |       |       |       |
| Q-factor        | 30            | 5.818 | 5.877 | 5.925 | 5.959 |
|                 | 40            | 4.512 | 4.544 | 4.569 | 4.588 |
|                 | 50            | 3.738 | 3.759 | 3.775 | 3.787 |
| <b>Cauchy</b>   |               |       |       |       |       |
| Q-factor        | 30            | 5.925 | 6.013 | 6.092 | 6.135 |
|                 | 40            | 4.569 | 4.616 | 4.658 | 4.681 |
|                 | 50            | 3.775 | 3.805 | 3.831 | 3.846 |
| <b>Sinc</b>     |               |       |       |       |       |
| Q-factor        | 30            | 5.877 | 5.959 | 6.013 | 6.051 |
|                 | 40            | 4.544 | 4.588 | 4.616 | 4.637 |
|                 | 50            | 3.759 | 3.787 | 3.805 | 3.818 |

### 8.2 The Q-factor

The obtained Q-factor after each stage is illustrated in Fig. 6 at different link lengths.

It is clear that Q-factor decreases with fiber length.

Table 5 summarizes all the Q-factor at all FBG stages. It is found that at the last stage, the Cauchy profile gives the best values of Q-factor: 6.135, 4.681 and 3.846 at distances 30 km, 40 km and 50 km, respectively.

### 8.3 BER

The BER obtained after each FBG stage of the proposed system is displayed in Fig. 7 at different link lengths.

Clearly, the BER increases with fiber length.

Table 6 summarizes the obtained BER at all FBG stages. It is found that at the last stage, the Cauchy profile gives the best BER: 4.24E-10, 1.43E-06 and 6.01E-05 at distances 30 km, 40 km and 50 km, respectively.

## 9 Proposed Model Evaluation

The proposed model is evaluated with the related work [14]. Figure 8 shows the evaluation for the proposed model with blue color and for the related work red.

For the proposed model, the spectral width,  $\Delta\lambda$ , in the best apodization function Cauchy is narrowed to 0.113 nm, 0.108 nm, 104 nm and 0.102 nm. For the related work [14], the design is able to narrow the optical spectrum significantly from 16 nm to around 8 nm and the  $-20$  dB bandwidth is decreasing slightly with the increase in the detuning



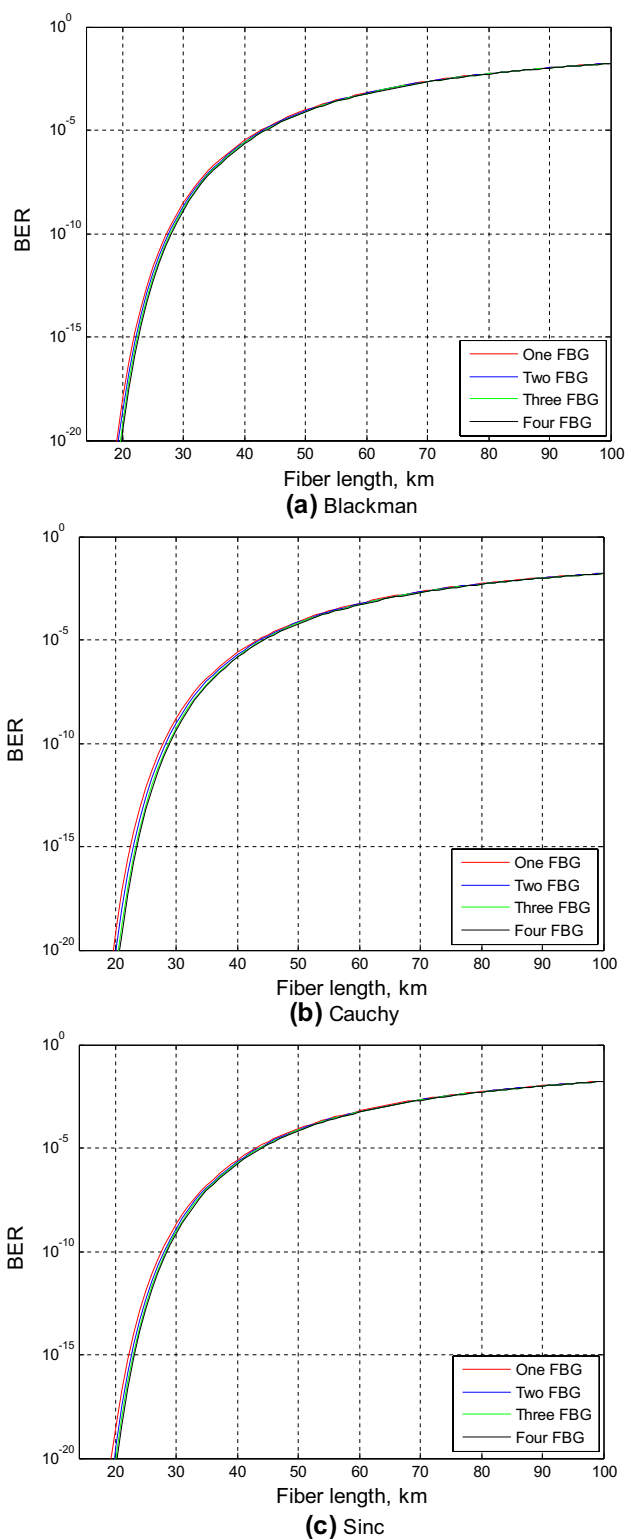


Fig.7 BER results for each stage a Blackman, b Cauchy and c Sinc apodization functions

Table 6 BER result after each stage

| Distance (km)   | 1st      | 2nd      | 3rd      | 4th      |
|-----------------|----------|----------|----------|----------|
| <b>Blackman</b> |          |          |          |          |
| BER 30          | 2.98E-09 | 2.09E-09 | 1.56E-09 | 1.27E-09 |
| 40              | 3.21E-06 | 2.76E-06 | 2.44E-06 | 2.24E-06 |
| 50              | 9.26E-05 | 8.54E-05 | 7.99E-05 | 7.63E-05 |
| <b>Cauchy</b>   |          |          |          |          |
| BER 30          | 1.56E-09 | 9.11E-10 | 5.56E-10 | 4.24E-10 |
| 40              | 2.44E-06 | 1.95E-06 | 1.59E-06 | 1.43E-06 |
| 50              | 7.99E-05 | 7.09E-05 | 6.36E-05 | 6.01E-05 |
| <b>Sinc</b>     |          |          |          |          |
| BER 30          | 2.09E-09 | 1.27E-09 | 9.11E-10 | 7.17E-10 |
| 40              | 2.76E-06 | 2.24E-06 | 1.95E-06 | 1.77E-06 |
| 50              | 8.54E-05 | 7.63E-05 | 7.09E-05 | 6.72E-05 |

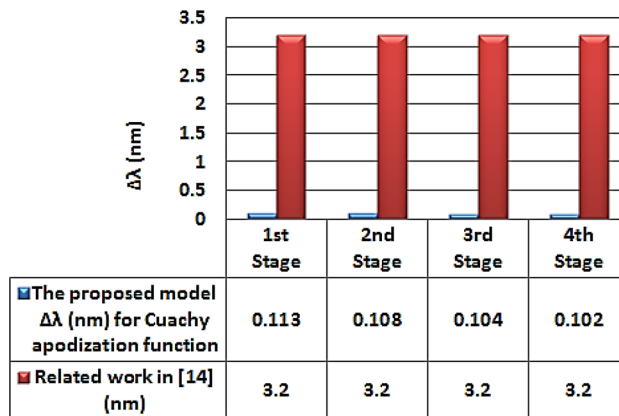


Fig.8 Proposed model evaluation

until around 3.2 nm. This comparison obviously assures that our proposed model achieves significantly a narrower spectral width.

## 10 Conclusion

In this paper, we proposed an FBG system that aims to reduce the used spectral width of the optical signal to reduce dispersion and improve system performance. Many apodization profiles are investigated. It is found that the Cauchy apodization function is the best one that reduces the reflective spectral width  $\Delta\lambda$  to 0.102 nm and achieves the best Q-factor at distances 30, 40 and 50 km which are 6.135, 4.681 and 3.846, respectively. In addition, it gives the minimum BER of  $4.24\text{E}-10$ ,  $1.43\text{E}-6$  and  $6.01\text{E}-5$ , respectively, at the same distances.

## References

- Seimetz, M., Markus, N., Erwin, P.: Optical systems with high-order DPSK and star QAM modulation based on interferometric direct detection. *J. Lightwave Technol.* **25**(6), 1515–1530 (2007)
- Ly, G., Kikuchi, T.: Coherent detection of optical quadrature phase-shift keying signals with carrier phase estimate. *J. Lightwave Technol.* **24**(1), 12–21 (2006)
- Payne, J.M., Shillue, W.P.: Photonic techniques for local oscillator generation and distribution in millimeter-wave radio astronomy. In: International Topical Meeting on Microwave Photonics, pp. 9–12. (2002).
- Trobs, M., Wessels, P., Fallnich, C.: Phase-noise properties of an ytterbium-doped fiber amplifier for the Laser Interferometer Space Antenna. *Opt. Lett.* **30**(7), 789–791 (2005)
- Kaltenegger, A., Fridlund, M.: The Darwin mission: Search for extra-solar planets. *Adv. Space Res.* **36**(6), 1114–1122 (2005)
- Petrou, V., Roudas, A.: Quadrature imbalance compensation for PDM QPSK coherent optical system. *IEEE Photon. Technol. Lett.* **21**(24), 1876–1878 (2009)
- Grote, N., Venghaus, H.: *Fiber OPTIC Communication Devices*. Springer, Berlin (2017)
- Agrawal, G.P.: *Fiber-Optic Communication Systems*. Wiley, London (2012)
- Keiser, G.: *Signal Degradation in Optical Fiber*. McGraw-Hill, New York (2000)
- Venghaus, H.: *Wavelength Filters in Fiber Optics*. Springer, Berlin (2006)
- Ducournau, B., Szriftgiser, P., Peytavit, Z., Lampin, N.: Cascaded Brillouin fibre lasers coupled to untravelling carrier photodiodes for narrow linewidth terahertz generation. *Electron. Lett.* **50**(9), 690–692 (2014)
- Seo, D.-S., Ha, T., Yong-Yuk, W.: Spectral width reduction of a laser source by external phase noise compensation. *Electron. Lett.* **55**(12), 703–704 (2019)
- Cliché, J.-F., Martin, A., Michel, T.: (2006) High-power and ultra-narrow DFB laser: the effect of linewidth reduction systems on coherence length and interferometer noise. In: *Laser Source and System Technology for Defense and Security II*, International Society for Optics and Photonics, vol. 6216. (2006)
- Junwei, F., Yanping, X., Xun, L., Wei-Ping, H.: Narrow spectral width FP lasers for high-speed short-reach applications. *J. Lightwave Technol.* **34**(21), 4898–4906 (2016)
- Karthick, S., Singh, S., Prabu, S.S.M., Khan, S., Agarwal, V., Chitkariya, P., Saxena, M.K., Venkatesh, R., Palani, I.A.: Influence of quaternary alloying addition on transformation temperatures and shape memory properties of Cu–Al–Mn shape memory alloy coated optical fiber. *Measurement* **153**, 107379 (2020)
- Tran, H., Guo, K., Morton, B.: Ring-resonator based widely-tunable narrow-linewidth Si/InP integrated lasers. *IEEE J. Sel. Topics Quant. Electron.* **26**(2), 1–14 (2019)
- Huang, D., Tran, M.A., Guo, J., Peters, J., Komljenovic, T., Malik, A., Morton, P.A., Bowers, J.E.: High-power sub-kHz linewidth lasers fully integrated on silicon. *Optica* **6**, 745–752 (2019)
- Kashyap, R.: *Fiber Bragg Gratings*. Academic Press, London (1999)
- Ashry, I., Elrashidi, A., Mahros, A., Alhaddad, M., Elleithy, K.: Investigating the performance of apodized fiber bragg gratings for sensing applications. In: *Conference of the American Society for Engineering Education*, Bridgeport, CT, USA, vol. 14, pp.1–5, 3–5. (2014)
- Mohammed, N., Ayman, W.E., Moustafa, H.A.: Distributed feedback fiber filter based on apodized fiber Bragg grating. *Optoelectron. Adv. Mater. Rapid Commun.* **9**(9–10), 1093–1099 (2015)
- Hanan, M.E.-G., Heba, A.F., Ahmed, A.E.-A., Moustafa, H.A.: Performance analysis & comparative study of uniform, apodized and pi-phase shifted FBGs for array of high performance temperature sensors *Optoelectron. Adv. Mater. Rapid Commun.* **9**(9–10), 1251–1259 (2015)
- Sayed, A.F., Barakat, T.M., Ali, I.A.: A novel dispersion compensation model using an efficient CFBG reflectors for WDM optical networks. *Int. J. Microwave Opt. Technol.* **12**(3), 230–238 (2017)
- Mohammed, N., Okasha, N.M., Aly, M.H.: A wideband apodized FBG dispersion compensator in long haul WDM systems. *J. Optoelectron. Adv. Mater.* **18**(5–6), 475–479 (2016)

**Publisher's Note** Springer Nature remains neutral with regard to jurisdictional claims in published maps and institutional affiliations.



**Ahmed F. Sayed** Works in Telecom Egypt Company in Egypt in the field of fiber optic communication in SDH, OTN, and DWDM equipments. He had a bachelor's degree in communications engineering from the faculty of engineering, Helwan University in Cairo and a master degree from faculty of engineering in Fayoum University. Ahmed F. Sayed: Works in Telecom Egypt Company in Egypt in the field of fiber optic communication in SDH, OTN, and DWDM equipments. He had a bachelor's degree in communications engineering from the faculty of engineering, Helwan University in Cairo and a master degree from faculty of engineering in Fayoum University.



**Fathy M. Mustafa** Received the B.Sc. degree in Electronics and communications department, in 2003. He is earned the M.Sc degree in Electronics and communication engineering from Arab Academy for Science and Technology & Maritime Transport College of Engineering and Technology, Alexandria, Egypt. He received his Ph.D in electrical engineering from Mina University. Her areas

of interest include optical communications, optical amplifiers and solar cells.



**Ashraf A. M. Khalaf** Received his B.Sc. and M.Sc. degrees in electrical engineering from Minia University, Egypt, in 1989 and 1994, respectively. He received his Ph.D in electrical engineering from Graduate School of Natural Science and Technology, Kanazawa university, Japan in 2000. He works at electronics and communications engineering Department, Minia University. He is a member of IEEE since 12 years.



**Moustafa H. Aly** Professor electronics and communications department, college of engineering, Arab Academy for Science, Technology and Maritime Transport. Field of interest optical communications, laser, optoelectronics, optical networks, engineering physics and optics. Research indicators Scopus URL, Google Scholar URL,

Research gate, Academia and LinkedIn. Member of the optical society of America (OSA).